

A MULTIPLE TARGET APPROACH FOR SINGLE QUANTUM DOT TRACKING

Stéphane Bonneau^{1,2}, Laurent Cohen¹, Maxime Dahan²

¹CEREMADE
Université Paris IX - Dauphine
75775 Paris, France

²Laboratoire Kastler-Brossel
Ecole Normale Supérieure de Paris
75005 Paris, France

ABSTRACT

Semiconductor quantum dots (QDs) are nanometer-sized fluorescent particles with a great promise for advanced biological imaging. They have recently been shown to be very favorable probes for ultrasensitive detection. When specifically attached to a biomolecule of interest, they allow for single molecule tracking in live cells over unprecedented durations and open new prospects for the study of cellular dynamics. We present an algorithm for automatically detecting and tracking QDs in sequences of fluorescence images. It accounts for the blinking in the fluorescence signal of individual QDs assuming brownian dynamics of the biomolecules. Our algorithm analyzes images sequentially and can be extended to a real-time use.

1. INTRODUCTION

Single molecule detection (SMD), combined to single particle tracking (SPT) is a novel approach to investigate the mobility of specific objects in heterogeneous systems such as biological media. In live cells, SPT has been often used to study the membrane dynamics of proteins or lipids [1, 2] specifically attached to a probe. To truly access single-molecule properties and not alter the dynamics of the biomolecules, the ideal probe should give a bright optical signal and be as small as possible. Among the fluorescent labels used in recent years, semiconductor QDs appear specially promising for their small size (5 to 15 nm), brightness and photostability [3].

Recently, QDs have been used to monitor the diffusion of individual glycine receptors in cultured neurons [4]. QDs were shown to provide high signal to noise ratio and allowed continuous data acquisition for durations of at least 10-20 minutes, previously inaccessible with other fluorescent labels. For this experiment, live cells were observed with an epifluorescence microscope. The light emitted by QDs at wavelength $\lambda = 605$ nm was spectrally filtered and collected on a 16-bit CCD camera. Sequences of up to 1000

consecutive images (128×128 pixels) were acquired with an integration time of $t_{\text{int}} = 75$ ms (Fig. 1.A).

To extract the relevant biological information from these data, a method is required to automatically detect and track single QD-tagged molecules. This is a challenging task : fluorescence images are particularly noisy (high spatial and temporal resolution limits the amount of photons available for detection) and the light emitted by single QDs blinks in a random manner [5]. Among the methods already proposed to track objects in dynamic fluorescence microscopy [6, 7, 8], none was dedicated to detect and follow multiple punctual objects which disappear and reappear after a potentially long extinction period. In this paper, we present an algorithm to monitor tagged molecules on the fly. Our method allows the tracking of an unknown number of targets and could be straightforwardly extended to a real-time use. Fluorescent images are analyzed sequentially and our scheme is split in two main steps. First, in the detection stage, fluorescent spots are detected by cross-correlation. Then, in the association stage, the set of trajectories is updated assuming brownian dynamics of the biomolecules.

2. DETECTION STAGE

2.1. Fluorescence image model

The size of a QD being much smaller than its wavelength λ , it acts as a point source of light. The response of the optical system (the point spread function, PSF) can thus be approximated by an isotropic 2D Gaussian function with a standard deviation $s = R_A/3$, where $R_A \approx 1.22\lambda/2N_A$ denotes the Airy radius and N_A the numerical aperture. For our setup, the pixel size is $a = 216.7$ nm and $N_A = 1.45$, so $s \approx 84.84$ nm ≈ 0.39 pixel. Neglecting motion of the QDs during acquisition, a fluorescent image is a snapshot of the sample at a given time and results from the convolution of the PSF with the spatial distribution of point sources (Fig. 1.A and Fig. 1.B).

The intensity of each pixel in an image corresponds to the number of detected photons added to a constant baseline offset L_B . We assume that fluorescence images are af-

Thanks to Ministère de la Recherche (DRAB Program) and CNRS for funding.

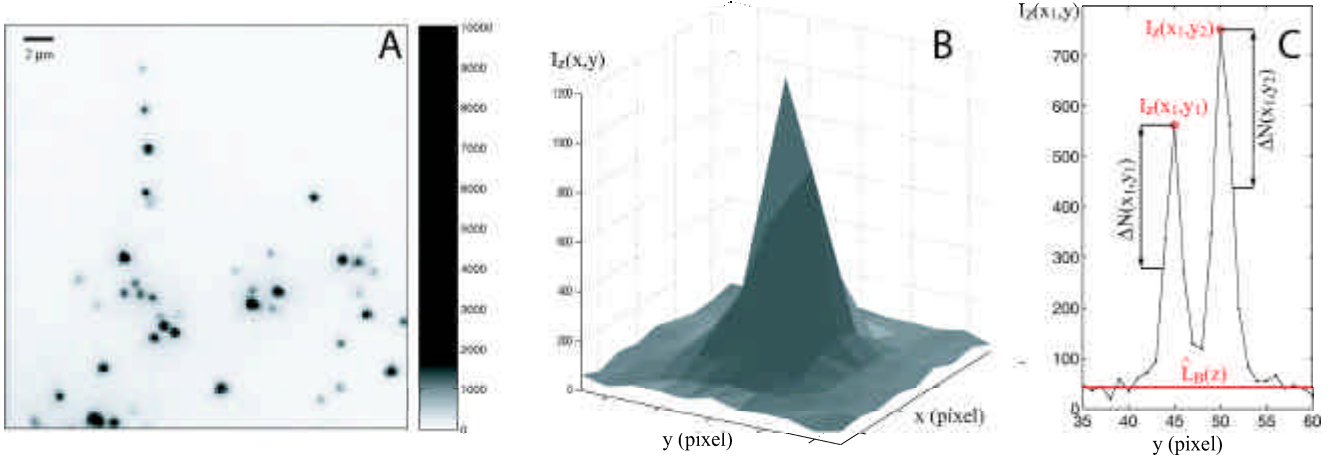


Fig. 1. (A) A typical fluorescence image. The inverted gray scale map is shown on the right. (B) A fluorescent spot results from the convolution of the PSF with a point source. (C) Illustration of the peak selection on a fluorescence image profile. The two spot candidates (located along the same line x_1) pass the detection test.

ected by the superposition of two independent noises : shot noise and dark noise [9]. Shot noise, due to the quantum nature of light, is Poisson distributed with a variance equal to the number of detected photons. Dark noise refers to the noise caused by background photons, CCD readout noise and dark current. We model it by an additive zero-mean gaussian distribution with a variance σ_B^2 independant of the number of detected photons. Let us note I_z the z^{th} frame of the image sequence and $I_z(x, y)$ the intensity of the pixel of coordinates (x, y) . The uncertainty in the intensity $I_z(x, y)$ is given by : $\text{var}[I_z(x, y)] = (I_z(x, y) - L_B) + \sigma_B^2$.

2.2. Estimation of the background and σ_B

Let us assume that most of the pixels of I_z represent image background. It is not a strong assumption if the concentration of dye molecules is moderate.

First, we extract from I_z an estimate $\widehat{L}_B(z)$ of the background. We compute a mean image \bar{I}_z by averaging each pixel value of I_z in a $M_x \times M_y$ neighborhood, i.e. we convolve I_z with a constant kernel h_1 : $\bar{I}_z = I_z * h_1$, so that $h_1(x, y) = 1/(M_x M_y)$ on its support. The mask size, motivated by the diameter of the PSF, is $M_x = M_y = 5$. The background value is expected to be the most represented intensity value of \bar{I}_z . So, we assign to $\widehat{L}_B(z)$ the intensity associated to the maximum of a smoothed histogram of \bar{I}_z . Note that $\widehat{L}_B(z)$ decreases over z due to the residual auto-fluorescence and asymptotically tends to the baseline offset L_B .

Let $I_z^\sigma(x, y)$ be the standard deviation of $I_z(x, y)$ in a $M_x \times M_y$ neighborhood. Thus $I_z^\sigma = [(I_z - \bar{I}_z)^2 * h_2]^{1/2}$ where $h_2(x, y) = 1/[(M_x - 1)(M_y - 1)]$ on its support. In

order to estimate the gaussian noise variance, one defines an auxiliary variable $\widehat{\sigma}_B(z)$, assigning to it the intensity associated to the maximum of a smoothed histogram of I_z^σ . Finally, we estimate σ_B by $\widehat{\sigma}_B(z)$, where $\widehat{\sigma}_B(z)$ is the mean value of $\widehat{\sigma}_B$ over the z already processed frames.

2.3. Template matching and peak selection

The fluorescent spots we want to detect present two convenient properties : they are isotropic and of known spread. For such a template matching, one of the most efficient method is the normalized cross-correlation. In our case, the template is the PSF, i.e. an isotropic 2D Gaussian function with standard deviation s , discretized on a support of size $M_x \times M_y$. Let us note PSF_G this template, $\overline{\text{PSF}_G}$ its intensity mean over the support and PSF_G^σ its intensity standard deviation. The normalized cross-correlation image γ_z is computed in the following manner (here \star denotes the correlation operator) :

$$\gamma_z = \frac{(I_z - \bar{I}_z) \star (\text{PSF}_G - \overline{\text{PSF}_G})}{[(M_x - 1)(M_y - 1)]^2 I_z^\sigma \text{PSF}_G^\sigma}$$

Note that computing \bar{I}_z , I_z^σ and γ_z in the the Fourier domain using FFT is fast enough to be done in real time. The function γ_z is a similarity measure between the template PSF_G and the fluorescent image I_z . To obtain a set of candidate spot locations, we apply to γ_z a local maximum detection in a $M_x \times M_y$ neighborhood.

Some correlation maxima are due to noise in the fluorescence image, so one needs to select the most reliable ones among the set of candidate spot locations. Let (x_m, y_m) be the coordinates of one of the correlation maxima. We can

estimate the uncertainty in the intensity $I_z(x_m, y_m)$ by :

$$\text{var}[I_z(x_m, y_m)] = (I_z(x_m, y_m) - \widehat{L}_B(z)) + \widehat{\sigma}_B^2(z).$$

Let $\Delta N(x_m, y_m) = k \sqrt{\text{var}[I_z(x_m, y_m)]}$ be a confidence interval so that k is a detection threshold corresponding to the minimal SNR that spots must satisfy to be detected. One decides there is a spot located at (x_m, y_m) if (Fig. 1.C) : $[I_z(x_m, y_m) - \Delta N(x_m, y_m)] > \widehat{L}_B(z)$.

2.4. Spot location refinement

In order to get a rapid subpixel estimate of the position of each detected spot, we apply a three point estimator on directions x and y . Let (x_m, y_m) be the pixel coordinates of a detected spot. The subpixel coordinate of that spot along the x -axis, denoted x_0 , is estimated according to the following relation, based on the assumption that a spot is gaussian :

$$x_0 = x_m + \frac{I_{(-1,0)}^{\max} - I_{(1,0)}^{\max}}{2 I_{(-1,0)}^{\max} - 4 I_{(0,0)}^{\max} + 2 I_{(1,0)}^{\max}}$$

where $I_{(i,j)}^{\max} = \log [I_z(x_m | i, y_m | j) \widehat{L}_B(z)]$. The same process is led on the orthogonal direction, in order to get a subpixel coordinate y_0 . The accuracy of the three point estimator, evaluated from Monte-Carlo simulations, is about 20 nm (1/10 pixel) along each axis. A more accurate localization can be obtained, at the expense of additional computing time, using a full least-squares gaussian fit [9].

3. ASSOCIATION STAGE

Once spots are detected on the image I_z , the next task is to associate them to the already estimated trajectories. We use a model of the dynamics in order to predict the possible location of spots in the neighbouring images of the sequence.

3.1. Receptor dynamics model

Early models of the plasma membrane (notably the fluid mosaic model) postulated that proteins, homogeneously distributed within the membrane, move by free diffusion in a lipid bilayer. Whereas SPT experiments have revealed a large diversity in the motion of individual molecules, let us apply Occam's razor principle and assume that the receptor dynamics is a planar Brownian motion.

In an homogeneous two-dimensional system, the probability distribution C that a particle with a diffusion coefficient D suffers a displacement r in a time period τ is [1] :

$$C(r, \tau, D) = \left(\frac{1}{4\pi D\tau} \right) \exp \left(- \frac{r^2}{4D\tau} \right).$$

In SPT experiments, one measures the successive positions $\mathbf{r}(t) = [x(t), y(t)]$ of the label molecule. The diffusion coefficient can be evaluated by means of the mean square displacement (MSD) function defined by :

$$\rho(\tau) = \left\langle \|\mathbf{r}(t + \tau) - \mathbf{r}(t)\|^2 \right\rangle = 4D\tau.$$

3.2. Application to receptor tracking

Data association is fundamental when dealing with multiple targets : new measurements on the image I_z must be reliably associated to tracks built with the $(z - 1)$ first frames. Conventional association methods, as the Joint Probabilistic Data Association Filter (JPDAF) [10] or the heuristic techniques presented in [11], do not account for long disappearances of tracked objects. We present here a simple rule of data association based on the receptor dynamics model.

Let us note T the set of tracks built with the $(z - 1)$ first frames. To the k^{th} track of T , we assign the state vector $\theta_k = [\mathbf{r}_k, z_k, D_k]$ where $\mathbf{r}_k = [x_k, y_k]$ is the last known position of the k^{th} track on the plane z_k and D_k is its estimated diffusion coefficient (see below for details). Let us note S_z the set of spots detected on I_z . For the j^{th} spot of S_z , we have its position $\mathbf{r}_j = [x_j, y_j]$. In order to reduce the complexity of the correspondence problem, we accept matching between the k^{th} track of T and the j^{th} spot of S_z if the following conditions are both satisfied :

- **C1** The QD associated to the k^{th} track of T has not disappeared on more than Δ_z^{\max} frames, where Δ_z^{\max} is a persistence criterion a priori fixed : $(z - z_k) \leq \Delta_z^{\max}$.
- **C2** The probability that the QD associated to the k^{th} track diffused over a distance $d_{j,k} = \|\mathbf{r}_j - \mathbf{r}_k\|$ does not exceed $(1 - P)$, where P is a threshold probability a priori fixed. The following inequality must thus be satisfied : $d_{j,k} < \sqrt{4 D_k (z - z_k) t_{\text{int}} |\log(P)|}$.

The association stage algorithm is the following one :

1. Build the subset T_{C1} of T so that each track of T_{C1} satisfy **C1**.
2. Compute the euclidean distance between each spot of S_z and the last known position of each track of T_{C1} . Store each distance satisfying **C2** in a list $L_d^{(0)}$. Each element of $L_d^{(0)}$ gives the cost of an association between a spot and a track.
3. Apply the following sequential assignement scheme, which prevents tracks from fusing :
 $i := 0$
Do _____
 - Find $d_{j^*, k^*} = \min_{L_d^{(i)}} d_{j,k}$ (nearest neighbour)
 - Link the spot j^* to the track k^*

- $i := i + 1$
 - $L_d^{(i)} := L_d^{(i-1)} \setminus \{d_{j,k} \mid (j = j^*) \text{ or } (k = k^*)\}$
- until $L_d^{(i)} = \emptyset$

4. For each track to which a new point has been added, update the diffusion coefficient by applying a linear least-squares fit to an estimate of the MSD calculated over the last 30 positions [1, 12].
5. If some spots of S_z remain not-assigned, they are considered as new tracks, to which are given an arbitrary diffusion coefficient D_{ini} a priori fixed.

4. EXPERIMENTAL RESULTS

Our tracking method has been implemented in Matlab (Mathworks) on a 2.8 GHz Pentium IV and applied to sequences of fluorescence images. A few minutes are sufficient to analyse a complete image sequence of 1000 frames. Note that an implementation with a compilable language would allow a faster execution. Figure 2 shows some typical results, obtained with $\Delta_z^{\max} = 20$, $D_{ini} = 10^{-1} \mu\text{m}^2\text{s}^{-1}$, $P = 0.15$ and $k = 10$.

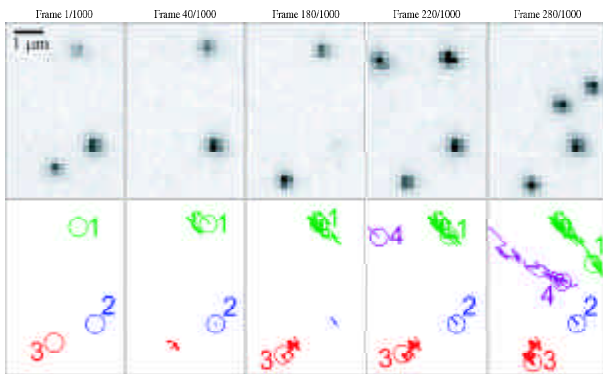


Fig. 2. Representative examples of molecular motions observed by single quantum dot imaging. First row : subregion (29×20 pixels) extracted from a fluorescence image sequence. Notice that some spots disappear and reappear. Second row : circles indicate detected spots and are surimposed to estimated trajectories.

5. CONCLUSION

Single particle tracking experiments require computational techniques to extract relevant biological information from long sequences of fluorescence images. We propose a fully automatic tracking algorithm, able to detect fluorescent spots and track them over time in an on-line approach. Our method is specially suitable for single quantum dot imaging, and accounts for the blinking of the fluorescent probes. The algorithm has been successfully applied to the analysis of the diffusion dynamics of membrane receptors in live neurons.

6. ACKNOWLEDGEMENTS

We are grateful to Sabine Lévi, Marie-Virginie Ehrensperger, Béatrice Riveau and Antoine Triller for providing us with experimental data and for valuable discussions on the analysis.

7. REFERENCES

- [1] Quian H. et al., “Single particle tracking : analysis of diffusion and flow in two-dimensional systems,” *Biophysical J.*, vol. 60, pp. 910–921, 1991.
- [2] Saxton M.J., “Single particle tracking : applications to membrane dynamics,” *Annu. Rev. Biophys. Biomol. Struct.*, vol. 26, pp. 373–399, 1997.
- [3] Chan W. et al., “Luminescent quantum dots for multiplexed biological detection and imaging,” *Curr. Opin. Biotechnol.*, vol. 13, pp. 40–46, 2002.
- [4] Dahan M. et al., “Diffusion dynamics of glycine receptors revealed by single quantum dot tracking,” *Science*, vol. 302, pp. 442–445, 2003.
- [5] Kuno M. et al., “On/off fluorescent intermittency of single semiconductor quantum dots,” *J. Chemical Physics*, vol. 115, pp. 1028–1040, 2001.
- [6] Tvarusko W. et al., “Time-resolved analysis and visualization of dynamic processes in living cells,” *Proc. Natl Acad. Sci. USA*, vol. 96, pp. 7950–7955, 1996.
- [7] Genovesio A. et al., “Tracking fluorescent spots in biological video microscopy,” *Proc. SPIE*, vol. 4964, pp. 98–105, 2003.
- [8] Sage D. et al., “Automatic tracking of particles in dynamic fluorescence microscopy,” *Proc. ISPA’03*, vol. 1, pp. 582–586, 2003.
- [9] Thomson R.E. et al., “Precise nanometer localization analysis for individual fluorescent probes,” *Biophysical J.*, vol. 82, pp. 2775–2783, 2002.
- [10] Fortmann T.E. et al., “Sonar tracking of multiple targets using joint probabilistic data association,” *IEEE J. Oceanic Engineering*, vol. 8, pp. 173–184, 1983.
- [11] Veenman C.J. et al., “Resolving motion correspondence for densely moving points,” *IEEE Trans. P.A.M.I.*, vol. 23, pp. 54–72, 2001.
- [12] Saxton M.J., “Single particle tracking : the distribution of diffusion coefficients,” *Biophysical J.*, vol. 72, pp. 1744–1753, 1997.